Space- and time-resolved Brillouin light scattering from nonlinear spinwave packets

O. Büttner, M. Bauer, A. Rueff, S.O. Demokritov, B. Hillebrands
Fachbereich Physik and Zentrum für Lasermesstechnik und Diagnostik, Universität Kaiserslautern, 67663 Kaiserslautern, Germany

A.N. Slavin
Department of Physics, Oakland University, 48309 Rochester, Michigan, U.S.A.

M.P. Kostylev, B.A. Kalinikos
St. Petersburg Electrotechnical University, 197376 St. Petersburg, Russia

We have constructed a new Brillouin light scattering apparatus, based on the Sandercock multipass tandem interferometer design, for space and time resolved investigations of nonlinear wave packets in thin films. We have applied the method to studies of nonlinear spin wave pulse propagation in yttrium iron garnet (YIG) films. Spatial resolution is achieved by scanning the laser spot across the YIG film surface, and temporal resolution is obtained by measuring the elapsed time between the launch of spin wave pulses by an applied microwave pulse and the arrival of the respective inelastically scattered photons at the detector. We report the observation of nonlinear self-focusing of wave beams and pulses in one and two dimensions, the formation of one-dimensional envelope solitons, and of strongly localized, two-dimensional wave packets, "spin wave bullets", analogous to "light bullets" predicted in nonlinear optics. By generating two counter-propagating wave pulses, pulse collision experiments were performed. We show that quasi-one-dimensional envelope solitons formed in narrow film stripes ("waveguides") retain their shapes after collision, while two-dimensional spin wave packets formed in wide YIG films are destroyed in collision.

1. Introduction

Brillouin light scattering (BLS) has developed to a very versatile tool to investigate thermally driven excitations, like phonons and spin waves, on surfaces and in films in the wavevector regime 0–10^5 cm^{-1} [1]. Light is inelastically scattered from these excitations, and by the determination of the frequency shift of the Doppler shifted light for a preset transferred wavevector, determined by the scattering geometry, the dispersion relation of the excitation is obtained. Of particular advantage of BLS are its high sensitivity, high spatial resolution determined by the diameter of the light focus on the sample surface (≈40 µm), high frequency resolution in the sub-GHz regime, high contrast and moderate costs of equipment. For surface and thin-film excitations, in particular in opaque materials, the tandem Fabry-Perot interferometer designed by Sandercock is now widely used as a fairly standard solution [2,3,4,5,6]. Here we report the extension of a tandem interferometer towards spatial and temporal resolution, enabling the investigation of the details of the propagation of travelling pulses of excitation. The method opens new fields of investigations. First, nonlinear excitations, like, e.g., microwave driven spin waves with large precession amplitudes in a magnetic film, can be monitored as they propagate through the film [7,8,9,10]. Pulses of surface phonons can be studied as well, although this is not subject of this manuscript. We are able to study the formation of spin waves in the vicinity of the exciting antenna, to determine the decay properties, reflection of spin waves at film boundaries, and the formation of waveguide patterns in laterally confined films. If the microwave field is large in amplitude, the excited spin waves are nonlinear, and nonlinear effects like, e.g., self-focusing and initial stages of wave collapse can be imaged [9]. Second, time resolution is added by measuring the elapsed time between the launch of a spin wave pulse in the film at the antenna position and the arrival of photons at the detector, which are inelastically scattered from the spin wave at the position of the laser focus.

We report the construction of a BLS setup with spatial and temporal resolution. We show results obtained for propagating spin waves in yttrium iron garnet (YIG) films in the nonlinear regime [7,8,9,10]. Phenomena like self focusing [7], formation of solitons in a quasi-one-dimensional waveguide and so-called spin wave bullets in infinite films [9] are presented. A crucial test to identify nonlinear objects are experiments, in which such objects collide in a head-on collision configuration [10]. Such experiments are reported.

2. Brillouin light scattering spectrometer

A tandem Fabry-Perot interferometer consists of two piezoelectrically controlled etalons each comprising two highly reflective, parallel mirrors as the frequency selecting elements. Light is transmitted by an etalon, if the mirror spacing L is a multiple of half the wavelength, λ. The tandem arrangement avoids ambiguities caused by the periodic transmission of light in each etalon. The basic layout of the instrument we are using is shown in Fig. 1. Light from a single-moded Ar^+ laser is focused with a lens on the sample mounted on a motor driven and computer controlled *xy*-translation stage. The scattered light is collected using an objective lens. The analyzer is used to suppress signals from phonons. The two spatial filters suppress background noise. The tandem arrangement of the etalons FP1 and FP2 is displayed in the right part. One of the two mirrors of each etalon is mounted on a common translation stage which is translated in the horizontal direction in Fig. 1 driven by a piezoelectic transducer. A change in spacing in δL in FP1 will result in a change in spacing $\delta L \cdot \cos(\theta)$ in FP2 with θ the angle between the two beam axes. If we assume that both

etalons are each in resonance, a change in δL by λ/2 will bring FP1 in the next transmission order, but FP2 will be off-resonance. By redirecting the light transmitted by FP1 into FP2 using a mirror, the light transmitted by FP1 will now be suppressed by FP2, and, by scanning the translation stage, an unambiguous assignment of inelastic peaks in the transmitted light intensity as a function of L to the frequency shift can be made in a straightforward manner. Multipassing the light yields the necessary high contrast of better than $1{:}10^{10}$, which is needed to discriminate the weak inelastic signals from the elastically scattered light. To achieve stable operation, a high degree of parallelity of the etalon mirrors and the correlation of the two etalons is maintained by an active stabilization scheme. We developed a computer controlled system taking advantage of a software solution, which performs the data accumulation and processing, the dynamic stabilization, as well as an automated alignment of the etalons prior to a measurement, and the execution of a pre-programmed series of measurements using a script language [6].

2.1 Space resolved Brillouin light scattering

The setup of a space resolved BLS apparatus is schematically shown in Fig. 2. Here spin waves are generated by a microwave input antenna. If microwaves with a frequency ω_0 are applied to the input antenna, a spin wave is launched with a wavevector determined by the dispersion relation $\omega(q)$ of the spin wave. The spatial distribution is now measured by scanning the laser beam across the sample, which is done by the motorized sample mount. Since microwave excited spin waves exist in a wavevector regime $|q| < 1200$ cm^{-1} with the upper bound imposed by the width of the antenna, we investigate the light scattered in forward direction to achieve a high sensitivity in this low-wavevector regime. The bottom part of Fig. 2 shows a typical distribution of spin wave intensities in a film of width $w = 2$ mm. The attenuation of the spin wave intensity, as the wave propagates away from the antenna, is clearly seen by the changing gray scale values varying from white (high intensity) to black (low intensity). By averaging the spin wave intensity in the transverse direction for each distance from the antenna, thus simulating the output signal strength of a receiving antenna, a purely exponential decay is observed which can be monitored over a dynamic range of >65 dB. The superimposed structure seen in Fig. 2 is caused by the waveguide geometry [8]. Here at least the two lowest lateral width modes are excited, for which the transverse wavevector is quantized due to the finite width w of the waveguide [8]. Interference of these modes, which propagate with slightly different phase velocities, creates the observed patterns.

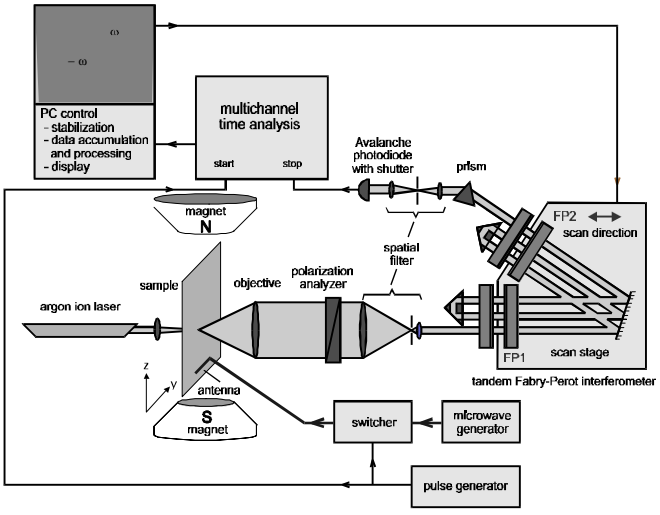

Fig. 1: Schematic layout of the Brillouin light scattering apparatus with space and time resolution. For a discussion of the components see the main text.

2.2 Time resolved Brillouin light scattering

Temporal resolution is easily added by using a time correlated single photon counting method similar to time-of-flight measurements in, e.g., mass spectroscopy. The complete setup is shown in Fig. 1. The tandem interferometer part was already discussed above. A pulse generator generates pulses of typically 10–30 ns duration with a repetition rate of 1 MHz. The pulse is sent to a microwave switcher device, to create a pulsed microwave field and to generate a spin wave pulse of same duration at the antenna. The output from the pulse generator is also used to start a 24 bit reference counter counting the output pulses of a 1.2 GHz time base. If the spin wave pulse crosses the laser spot, light is inelastically scattered, and the output signal of the photon detector is used to stop the reference counter. The counter content is now a measure of the elapsed time between spin wave launch and arrival at the position of the laser spot on the sample. A memory cell of a memory array addressed by the content of the counter is incremented by one and the procedure is repeated. After accumulating a large number of events the

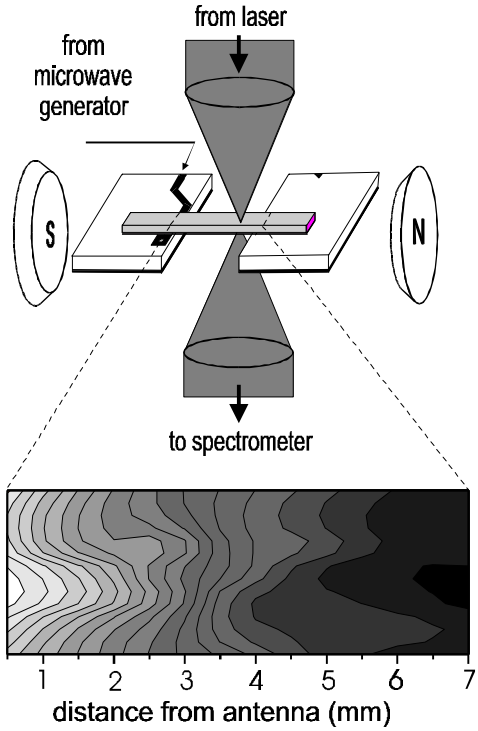

Fig. 2: Scheme of space resolved Brillouin light scattering. The laser beam is scanned across the sample, using a motorized *xy*-stage for the sample positioning, and the intensity of the light inelastically scattered from the spin waves is recorded. The intensity distribution of a $Lu_{2.04}Bi_{0.96}Fe_5O_{12}$ (BIG) film with a film thickness of 1.5 µm is shown in the lower part. The gray scale represents the logarithmic intensity with white (black) indicating high (low) spin wave intensity.

content of the memory array represents the temporal variation of the spin wave intensity at the current position of the laser spot. By repeating the procedure for each position of the sample, a two-dimensional map of the spin wave intensity is constructed for each value of delay time. We arrange the data in a digital video animation with each frame representing the spatial distribution of the spin wave intensity for a given delay time [11]. The entire system is realized in a digital signal processing device which interacts with a PC via an RS232 connection. The device can handle up to $2.5 \cdot 10^6$ events per second continuously. A lower bond of about 2 ns on the time resolution is imposed by the intrinsic time resolution of the etalons and the multipass arrangement in the BLS spectrometer [12]. Typical accumulation times are 5 seconds per position of the laser spot. A complete investigation of a YIG film with a sampling area of 2×6 mm^2 and a mesh size of 0.1 mm takes little more than two hours including dead times caused by sample positioning.

3. Nonlinear spin waves in a magnetic film

Nonlinear spin waves are an excellent testing ground to study the propagation of nonlinear waves in dispersive, anisotropic and dissipative media. As contrary to light waves in a medium, the spin wave dispersion and nonlinearity are fundamental properties of the Landau-Lifshitz equation of motion. Anisotropy is induced by the direction of magnetization and the dependence of the spin wave frequencies on the angle between the magnetization $\vec{M}$ and the wavevector $\vec{q}$. For a review of spin wave properties see, e.g. [13]

The dynamic properties of these systems are generally described by a nonlinear Schrödinger equation of the form:

$$i\left(\frac{\partial \varphi}{\partial t} + V_g \frac{\partial \varphi}{\partial z}\right) + \frac{1}{2} D \frac{\partial^2 \varphi}{\partial z^2} + S \frac{\partial^2 \varphi}{\partial y^2} - N |\varphi|^2 \varphi = -i\omega_r \varphi \quad (1)$$

where V_g is the group velocity, D is the dispersion and S is the diffraction coefficient, N is the nonlinear and ω_r is the damping parameter. φ is the dimensionless spin wave amplitude and z is the propagation direction. Solving this equations for different boundary conditions leads to solitons, self focusing and similar nonlinear phenomena.

4. Propagation of magnetic envelope solitons

Of particular interest are magnetostatic backward volume waves (MSBVW), which are dipolar spin waves travelling parallel to the in the film plane applied external field. For these waves dispersion is negative, and the so-called Lighthill-criterion [14] as a mandatory condition for the existence of nonlinear effects is fulfilled: both diffraction and dispersion are compensated by the nonlinear term in Eq. (1) for large enough amplitudes φ. In a one-dimensional waveguide so-called magnetic envelope solitons are formed [15] which were first observed by microwave experiments [16]. It is commonly believed, that the one-dimensionality of a waveguide structure is achieved if the width of the film is small compared to the wavelength of the spin wave excitation. Solitons in such a structure are expected to show a secans-hyperbolicus-like shape along the propagation direction, and a sine-like variation in the transverse direction, to

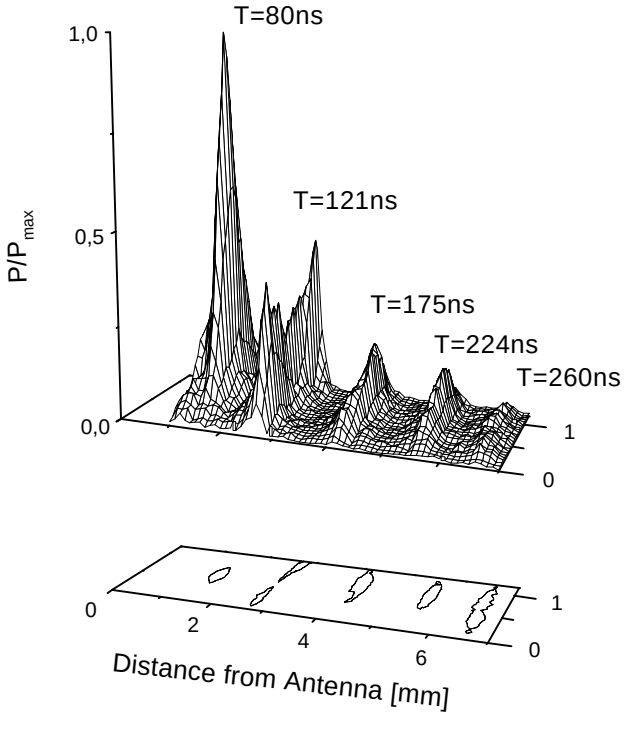

Fig. 3: Two-dimensional distributions of the normalized intensities of propagating solitons, corresponding to five different values of the propagation time as indicated in the figure. The input antenna is at the left side. The distributions were experimentally measured by the space- and time-resolved BLS technique for $\tau = 20$ ns and $P_{in} = 700$ mW. The film width is 2.3 mm, and the carrier wavenumber is 70 cm^{-1}. The cross-sections of the propagating wave-packets taken at half-maximum power are shown on the plane below.

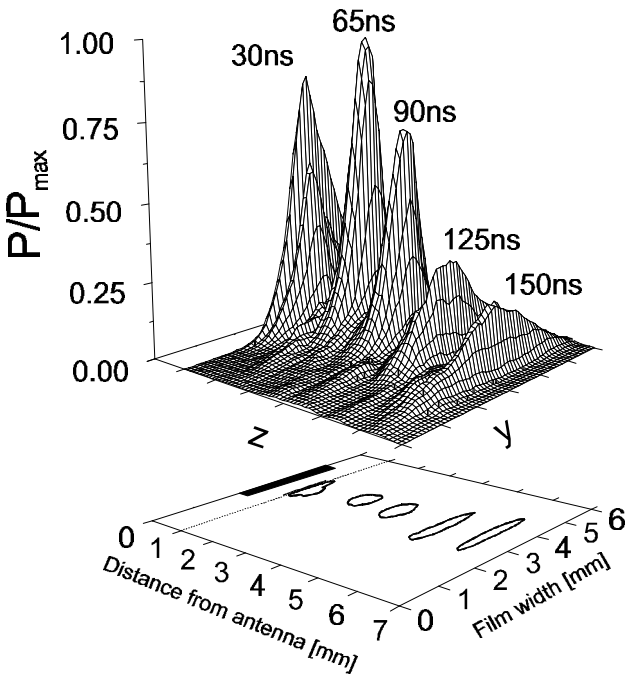

Fig. 4: Two-dimensional distributions of the normalized intensities of propagating dipolar spin wave packets, corresponding to five different values of the propagation time as indicated in the figure. The input antenna is indicated at the left side. The distributions were experimentally measured by the space- and time-resolved BLS technique for $\tau = 29$ ns and $P_{in} = 460$ mW. The cross-sections of the propagating wave-packets taken at half-maximum power are shown on the plane below. The area near the antenna is inaccessible by BLS, as indicated by the dotted line.

match the boundary conditions at the film side walls.
Using space and time resolved BLS the formation and propagation of a soliton can be easily studied. Figure 3 shows the intensity distribution measured at five different delay times. The lower part of the figure shows the cross section at half maximum of each peak. The carrier wavenumber is 70 cm^{-1}, the pulse width is 20 ns, and the input power at the antenna is 700 mW. The spin wave intensity was measured across the sample in an area of 1.5×6 mm^2 with a mesh size of 0.1 mm. At each point the complete time response of the local variable magnetization caused by the propagating spin wave was measured. It is immediately evident that the expected sine-like variation of the spin wave intensity along the *y*-axis is only achieved after initial formation of the soliton. In the formation regime (T = 80 ns in Fig. 3) self-focusing is observed. A detailed analysis of the data, as partially displayed in Fig. 3, yields a stable soliton propagation for 100 ns < T < 260 ns.

5. Propagation of spin wave bullets

We now discuss the propagation of nonlinear BVMSW modes in an infinitely extended film [9]. A soliton cannot exist anymore since for the type of nonlinearity used in Eq. (4) no stable eigen-solution exists in two spatial dimensions [17]. We show, however, that a new type of quasi-stable excitation appears, which is called a magnetic bullet in analogy to light bullets first prediced by Silberberg in the case of nonlinear light pulses. Simple models based on the nonlinear Schrödinger equation show, that self-focusing may lead to a collapse of the initial wave packet, when the packet amplitude becomes infinite in a finite time [18]. In the real physical world this is, of course, avoided, and the process of collapse is stopped at some point by saturation of nonlinearity and/or by dissipation. As a result, stable, so-called bullet excitations are predicted [19]. Here we report on the first experimental observation of such a bullet excitation, which is a spin wave bullet in a two-dimensional magnetic YIG film [9].

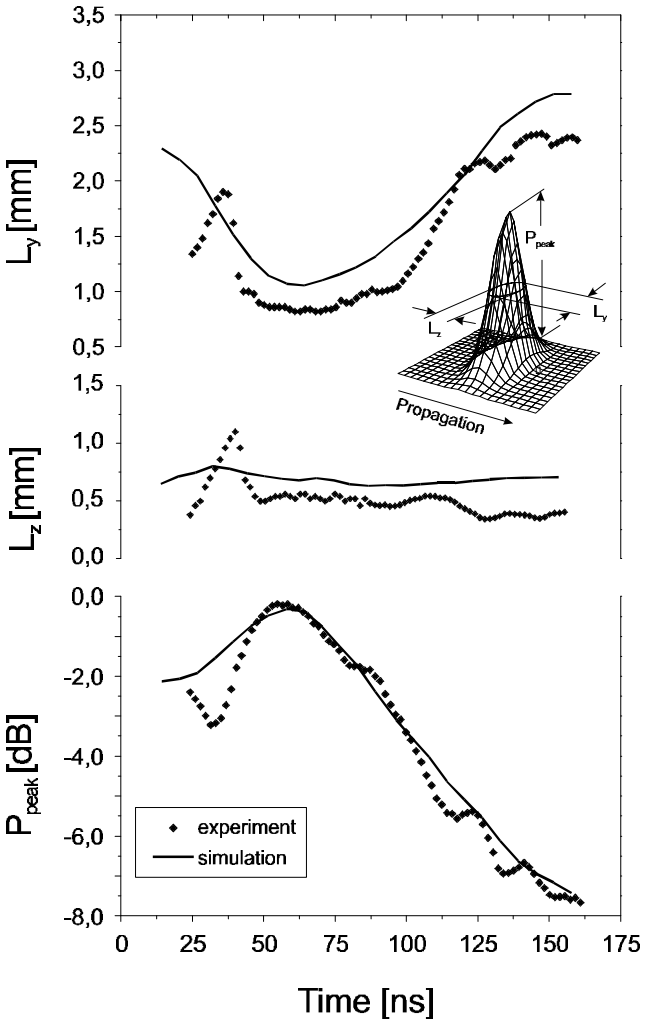

Fig. 5: Transverse and longitudinal pulse widths L_y and L_z at half maximum power, and normalized peak power of the propagating spin wave packet shown as functions of the propagation time T for $\tau = 29$ ns and $P_{in} = 460$ mW: symbols: experiment, lines: numerical simulation.

For our experiments we used a large YIG sample (18x26 mm^2) with a film thickness of 7 µm, which was mounted on a microstrip antenna with a length of 2.5 mm and a width of 50 µm. The applied magnetic field, which was aligned along the propagation direction of the pulses, was 2098 Oe. The carrier wave number of the excited backward volume magnetostatic spin wave (BVMSW) modes was 50 cm^{-1}. The pulse length for the experiment, which is discussed below, was $\tau = 29$ ns, the microwave input power was between 10 and 700 mW. The other conditions are as in the case of envelope solitons discussed above.
Fig. 4 shows the results for a microwave input power of 460 mW. The peaks in the figure show the pulse shapes measured at five different delay times T as indicated at the peaks. The cross sections of the pulses are shown in the lower part of Fig. 4. The pulse is forming for $T < 40$ ns. Subsequently it is focused in both spatial directions and then it forms a spin wave bullet. The bullet now propagates for ≈60 ns without a significant change of its shape, thereby loosing energy evidenced by the decay of its amplitude. This can be more clearly seen in Fig. 5, which shows the width of the pulse perpendicular to the direction of propagation (L_y), and in the direction of propagation (L_z) as well as the maximum amplitude of the pulse (P_{peak}) as a function of time. After the pulse has lost too much energy the amplitude is below the threshold for stabilization, and, like a linear pulse, it decays due to diffraction, dispersion and dissipation. This can be seen in the increase in the pulse width in Fig. 5.
These findings can be modeled using the two-dimensional nonlinear Schrödinger equation, Eq. (1). The results are shown for comparison in Fig. 5. As can be seen the main features of the pulse propagation are in good qualitative agreement with the experiment.

6. Head-on collision of spin wave solitons and bullets

A crucial test for the presence of a soliton-like excitation is the behavior of these excitations upon head-on collision. Collision experiments are easily performed using space and time resolved BLS and two input antennas to create the two counter-propagating excitations. We have performed studies of the collision properties of both solitons and spin wave bullets [10].
For our experiments we used either wide (18x26 mm^2, bullets) or narrow (1.5x15 mm^2, solitons) YIG samples with a film thickness of 7 µm and 5.9 µm, which were mounted on

two microstrip antennas with a length of 2.5 mm and a width of 50 µm separated by 8 mm. The applied magnetic field, which was aligned along the propagation direction of the pulses, was chosen between 2.0 and 2.1 kOe. The carrier wave number of the excited BVMSW modes was varied in the interval 50–100 cm^{-1}. In the chosen scattering geometry BLS was sensitive to modes with wave vectors up to $\approx 10^4$ cm^{-1}. The pulse length was $\tau = 29$ ns for bullets and $\tau = 20$ ns for solitons. The microwave input power was varied between 10 mW and 10 W per antenna. The spin wave intensity was measured across the sample in steps of 0.1 mm. At each point the complete time response of the local variable magnetization caused by the propagating spin wave was measured.

Figures 6 and 7 show the profiles of the BLS intensity, which is proportional to the square of the spin wave precession angle, in the colliding packets (upper parts) and their cross-section taken at a half-maximum (lower parts) at different delay times *T* as indicated.

Figure 6 corresponds to a narrow sample and demonstrates the collision of two envelope solitons. The figure clearly shows that after 100 ns, long before the collision, quasi-one-dimensional solitons are formed, i.e., the packets fill the full width of the sample. In the collision region a spin wave packet is formed, its longitudinal width being close to that of each of the solitons before collision. After the collision one observes two packets with almost the same shape as before the collision, which move away from each other. The observed scenario is in agreement with numerical simulations, directly based on the Landau-Lifshitz equation [20]. The situation in the quasi-two-dimensional case is illustrated by Fig. 7. Here the colliding objects are spin wave bullets. It demonstrates that two bullets, strongly localized in both directions, are formed before the collision. During the collision an even much narrower packet is created. However, after the collision the bullets are completely destroyed and one observes shapeless, rapidly decaying packets.

7. Conclusions

By adding space and time resolving capabilities to tandem Fabry-Perot interferometry a very versatile instrumental tool is obtained suitable to image propagating excitations in a magnetic field. We have discussed the detection of novel spin wave bullet excitations in an infinitely extended film, which is a nonlinear wave packet stabilized by dissipation. We have compared the properties of spin wave bullets to those of spin wave solitons in the quasi-one-dimensional case. We have shown that a crucial test for the properties of these nonlinear excitations is provided by the study of the collision scenario.

The power of space and time resolved BLS is not limited to spin waves. For example, surface phonons can be studied as well replacing the microwave antenna by a piezoelectric transducer or a laser pulse. The exploration of the potential of our technique is currently still at its beginning.

Acknowledgements

Support by the Deutsche Forschungsgemeinschaft is gratefully acknowledged.

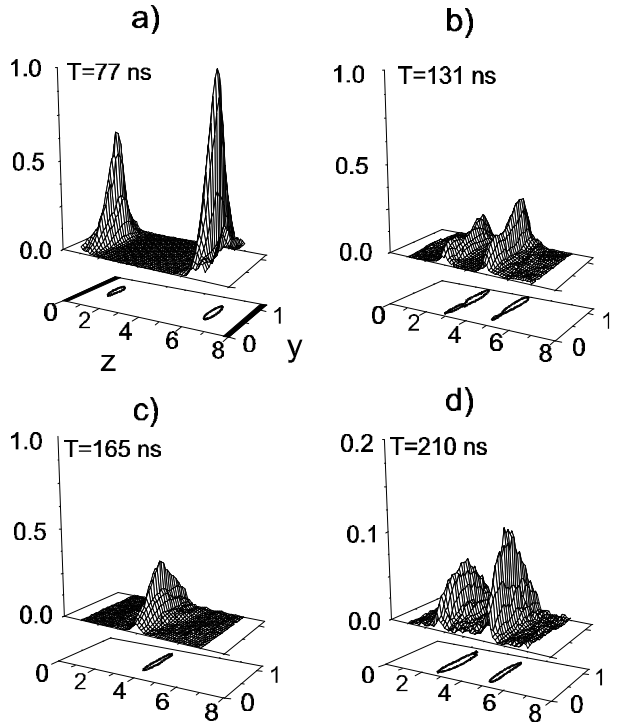

Fig. 6: The graphs show the normalized spin-wave intensity distribution of colliding spin-wave-packets in the quasi one-dimensional case (solitons) for different propagation times *T* as indicated in each graph. The lower part of each picture show the cross section of the pulses at half maximum. The microwave input power is 350 mW per antenna.

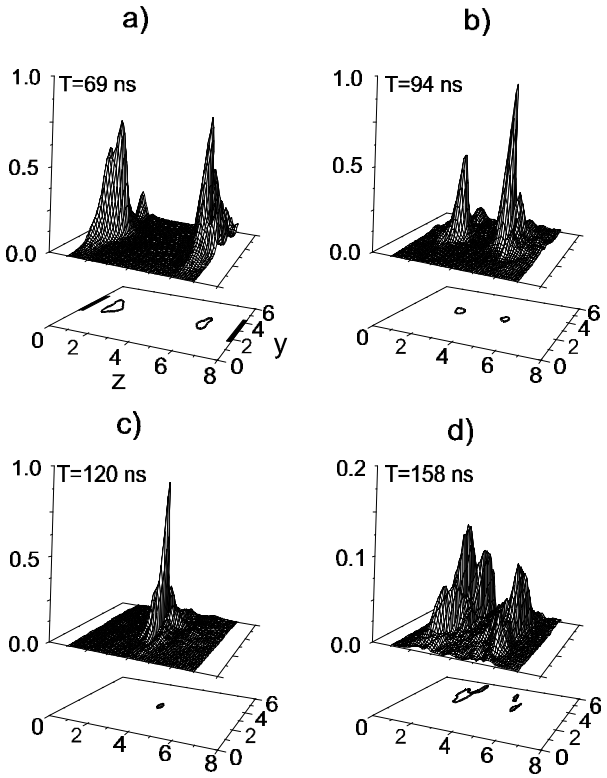

Fig. 7: The graphs show the normalized spin-wave intensity distribution of colliding spin-wave packets for the two-dimensional case (bullets) at different propagation times *T* as indicated in each graph. The microwave power is 2 W per antenna.

Reference

1 See, e.g., B. Hillebrands, *Brillouin light scattering from layered structures*, in: *Light Scattering in Solids VII*, M. Cardona, G. Güntherodt (eds.), Springer Verlag, Berlin, Heidelberg, New York, to appear in 1999, and references therein.

2 J.R. Sandercock, Solid State Commun. **26**, 547 (1978).

3 J.R. Sandercock, *Light scattering from thermally excited surface phonons and magnons*, Proc. 7th Int. Conf. on Raman Spectroscopy, W.F. Murphy (ed.), (North-Holland, Amsterdam), 364 (1980).

4 J.R. Sandercock, *Trends in Brillouin Scattering: Studies of Opaque Materials, Supported Films, and Central Modes*, Topics in Applied Physics **51**, Springer, Berlin (1982), p. 173.

5 R. Mock, B. Hillebrands, J.R. Sandercock, J. Phys. E **20**, 656 (1987).

6 B. Hillebrands, Rev. Sci. Instr. **70**, 1589 (1999).

7 M. Bauer, C. Mathieu, S.O. Demokritov, P. A. Kolodin, S. Sure, H. Dötsch, A. N. Slavin, B. Hillebrands, Phys. Rev. B **56**, R8483 (1997).

8 O. Büttner, M. Bauer, C. Mathieu, S.O. Demokritov, B. Hillebrands, P.A. Kolodin, M.P. Kostylev, S. Sure, H. Dötsch, V. Grimalsky, Yu. Rapoport and A.N. Slavin, IEEE Trans. Magn. **34**, 1381 (1998).

9 M. Bauer, O. Büttner, S.O. Demokritov, B. Hillebrands, Y. Grimalsky, Yu Rapoport, A.N. Slavin, Phys. Rev. Lett. **81**, 3769 (1998).

10 O. Büttner, M. Bauer, S.O. Demokritov, B. Hillebrands, M.P. Kostylev, B.A. Kalinikos, A.N. Slavin, Phys. Rev. Lett. **82**, 4320 (1999).

11 Video sequences in the AVI format can be downloaded from our home page http://www.physik.uni-kl.de/w_hilleb.

12 C.A. Eldering, A. Dienes, S.T. Kowel Optical Engeneering 32, 464 (1993)

13 'Linear and nonlinear spin waves in magnetic films and superlattices', M.G. Cottam (ed.), World Scientific, Singapore 1994

14 M.J. Lighthill, J. Inst. Math. Appl. 1, 269 (1965)

15 Since attenuation is not negligible the excitation should be called more precisely a quasi-soliton. It travels without change in shape until the amplitude is reduced by attenuation below the threshold for soliton formation.

16 B.A. Kalinikos, N.G. Kovshikov, A.N. Slavin, Sov. Phys. –JETP Lett. 38, 202 (1983)

17 V.E. Zakharov, A.M. Rubenchik, Sov. Phys. JETP 38, 494 (1974)

18 P.L. Kelly, Phys. Rev. Lett. **15**, 1005 (1965).

19 Y. Silberberg, Opt. Lett. **15**, 1282 (1990).

20 O. Büttner, M. Bauer, S.O. Demokritov, B. Hillebrands, M.P. Kostylev, B.A. Kalinikos, A.N. Slavin, Phys. Rev. Lett. 82, 4320 (1999).